ANALYTICAL PREDICTION OF CRACK RESISTANCE IN CONCRETE

A DISSERTATION

Submitted in partial fulfillment of the

requirements for the award of the degree

of

MASTER OF TECHNOLOGY

in

CIVIL ENGINEERING

(With Specialization in Structural Engineering)

By

MANOJ RAGHAV

(17523013)

DEPARTMENT OF CIVIL ENGINEERING

INDIAN INSTITUTE OF TECHNOLOGY ROORKEE

ROORKEE-247667 (INDIA)

MAY, 2019

CANDIDATE'S DECLARATION

I **Manoj Raghav** hereby declare that the work presented in this dissertation entitled **"ANALYTICAL PREDICTION OF CRACK RESISTANCE IN CONCRETE",** in partial fulfillment of the requirement for the award of the degree of **Master of Technology** submitted to Department of Civil Engineering **, Indian Institute of Technology Roorkee, India,** under the supervision of **Dr. SONALISA RAY** (Assistant Professor) Department of Civil Engineering, IIT Roorkee, is an authentic record of my work done during the spring semester of 2018-19. I have not submitted the matter embodied in this report for the award of any other degree or diploma.

Date:

Place: **Roorkee** **(MANOJ RAGHAV)**

CERTIFICATION

This is to certify that the above statement made by the candidate is correct to the best of my knowledge and belief.

Dr. SONALISA RAY
(Assistant Professor)
Department of Civil Engineering
IIT Roorkee

ACKNOWLEDGEMENT

I wish to express my deep sense of gratitude and sincere thanks to my guide **Dr. SONALISA RAY** (Assistant Professor) Department of Civil Engineering, IIT Roorkee, for being helpful and a great source of inspiration. I would like to thank her for providing me with an opportunity to work on this excellent and innovative field of research. Her keen interest and constant encouragement gave me the confidence to complete my work.

I wish to thank her for her constant guidance and suggestions without which I could not have successfully completed this report.

Date:

Place: Roorkee **(MANOJ RAGHAV)**

Table of contents

List of tables

List of figures:

ABSTRACT

Concrete is considered to be a heterogeneous material consisting of different phases comprising of aggregate, matrix and weak interfacial transition zone. Concrete has pre-existing microcracks in it and has quasi-brittle behavior. Concrete is different from ideal brittle materials because it has non-linear behavior in inelastic zone around the propagating crack. Fracture process zone is the result of this non-linear phenomena in concrete. The fracture zone governs the complete fracture behavior of concrete. Fracture process zone in concrete is complex due to various toughening mechanisms such as microcrack shielding, aggregate bridging, crack blunting etc.

The aim of this work is to understand the mechanism of formation and propagation of fracture process zone. Using the various numerical approaches, various fracture parameters like stress intensity factor and crack extension resistance has been determined, analyzed and compared under static and fatigue loading.

CHAPTER 1
INTRODUCTION

Concrete is a heterogeneous material having the quasi -brittle behavior and contain internal microcracks. Internal microcracks are the reason for the damage in concrete. Under load application, the internal microcracks grows in random direction and start to localize to form a major crack. The crack propagates up to the peak load in a stable manner and after the peak load, crack propagation becomes unstable exhibiting a gradual softening. Beyond the peak load, non-linear zone has been developed ahead of the crack tip.

Concrete has nonlinear response due to formation of fracture process zone (FPZ) ahead of the crack tip. It is the fracture process zone which effects the overall fracture behaviour of concrete. Fracture process zone is governed by various toughening mechanism such as crack deflection, crack branching, aggregate bridging etc. In this zone, new crack surfaces are formed and these surfaces have cohesive stresses which tends to close the crack. The cohesive stress in the fracture process zone is assumed to model the toughening mechanisms in the fracture process zone.[1]

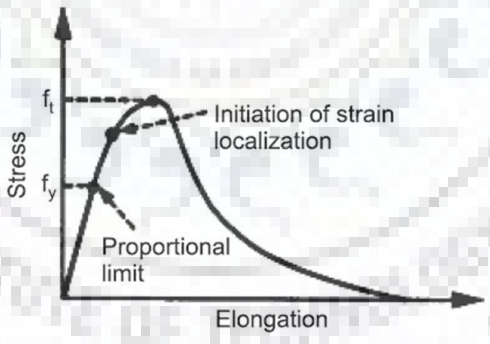

Figure 1.1: Quasi-brittle nature of concrete [1]

Fatigue is the process of weakening of concrete due to application of cyclic loads. It is a progressive structural damage. When the cyclic load reaches a certain threshold, crack will begin to form at notch tip. Fatigue life is the maximum no. of stress cycles that a concrete specimen can withstand without failure. The fatigue crack propagation in concrete is very complex because of various toughening mechanisms. Fatigue damage in concrete is also a non-linear process that exhibit transient crack stage and steady-state crack stage. Paris law has been

used to analyze fatigue damage in concrete. Paris law can also be used to measure the fatigue life [**2**].

In this report, we will study about crack propagation in concrete, evolution of fracture process zone and the fracture resistance of concrete. Variation of the fracture process zone (FPZ) length has been considered during the complete fracture process. To study the mechanism of fracture process zone (FPZ) and crack resistance of concrete, several numerical approaches are presented in this report.

1.1 Fracture mechanics in concrete

Fracture mechanics is the study of fracture of the material due to propagation of crack. In other words, resistance of a material to crack propagation is analyzed. Behaviour of concrete under loading is completely different from ductile materials. Concrete is considered as a quasi-brittle material. Many internal cracks exist in concrete prior to loading. The fracture behavior of concrete depends on when and how these internal cracks initiates and propagate under different loading condition.

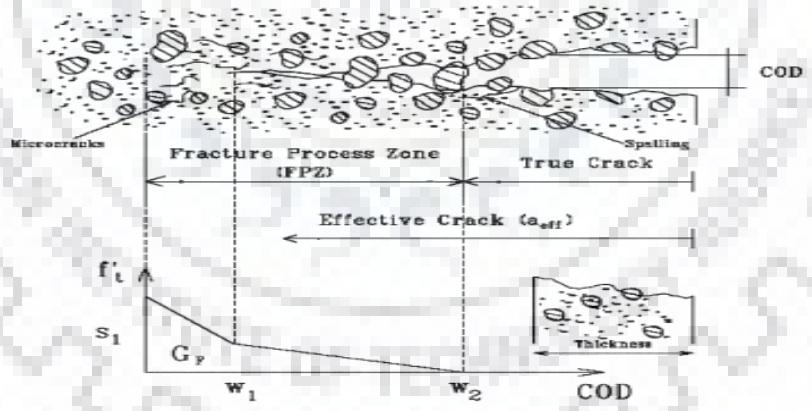

Figure 1.2: Fracture process zone [1]

The stress-strain curve is always linearly elastic up to the maximum stress for an ideally brittle material but for a quasi-brittle material like concrete there is significant non-linearity before the maximum stress. Strain softening can be observed under stable propagation of the crack. If a closed loop displacement-controlled test machine is used, both opening of the crack and unloading of the specimen can be observed for post peak part of the stress-strain curve **[1]**.

When external load is applied on the concrete, all the microcracks localizes to form a major crack and starts to propagate. The fracture process zone is made up of these microcracks. It is the region between cracked and uncracked portion. There are different toughening mechanisms exist in the fracture process zone of concrete to consume energy. Some of them are indicated below in Figure 1.3.

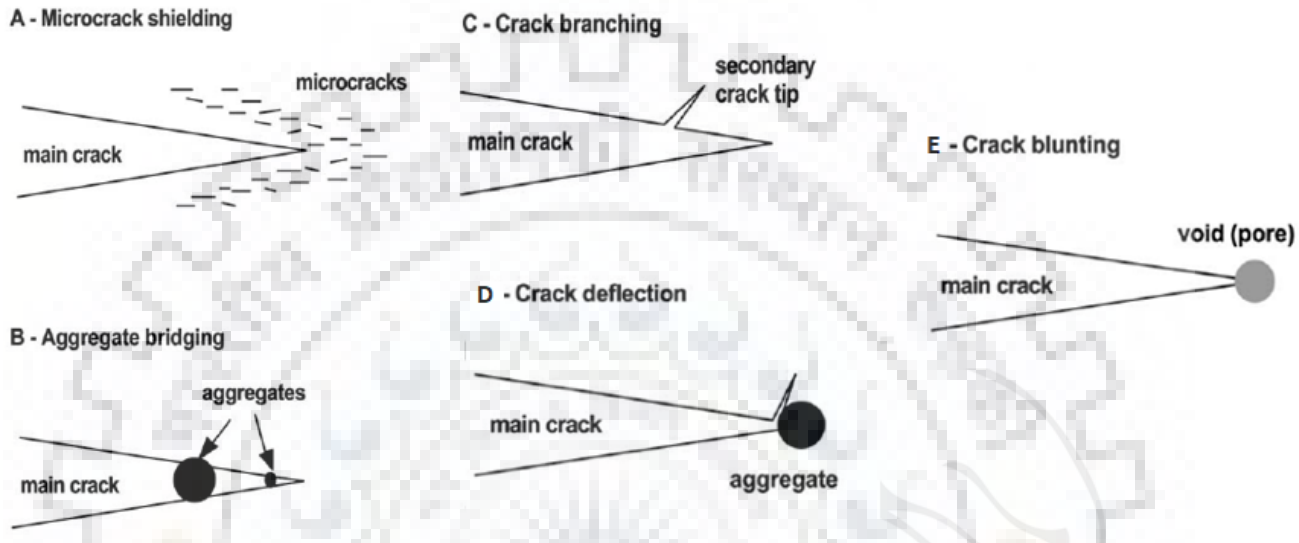

Figure 1.3: Various toughening mechanism in FPZ [1]

Specimen size and aggregate size also affects the fracture process zone. Greater the aggregate size, smaller and wider will be the fracture process zone. This zone deserves a special notice because it is very helpful to predict the ultimate failure in concrete and propagation of crack. In steel fracture process zone is very small and therefore strain hardening dominates over strain softening but in concrete fracture process zone is large and contain microcracks. So, strain softening dominates here.

1.2 OBJECTIVES

The objectives of the study is to calculate, analyses and compare the various fracture parameters under Static as well as in Fatigue loading from data obtained from 3-point bend test experiment. The objectives are as follows:

1. To find various fracture parameters like fracture toughness, stress intensity factor and crack extension resistance (K_{ini}, K_R) in concrete under 3- point bending static test and fatigue test.
2. To study load Vs CMOD and load Vs displacement curve.
3. To study the behavior of crack extension resistance curve throughout the process in static and fatigue loading.
4. To study fracture process zone length variation under loading throughout the process.
5. To determine Paris law constants from data obtained.

CHAPTER 2
LITERATURE REVIEW

In this chapter, literature review has been done for understanding the mechanism of formation and propagation of fracture process zone. Various numerical approaches and analytical model have been discussed in this chapter to determine fracture parameters like stress intensity factor and crack extension resistance under static and fatigue loading. As fracture process in concrete is very complex phenomena and tough to understand, therefore, a literature study is necessary to have a better idea of fracture terminologies under loading conditions.

Otsuka et al. [3] discusses about the shape of fracture process zone (FPZ). They studied about the impact of specimen size and aggregate on the fracture process zone. They also studied about the mechanisms to develop the fracture process zone and presented some concepts about fracture process zone. Several microcracks were observed ahead of the notch tip. This microcrack zone was considered as the major portion of the FPZ. When the loading increases from 0 to 30% of the peak, microcrack near the notch tip starts grow in random directions, from 30% to 70% of peak load, these microcracks starts to interconnect with each other, after 70% of the peak load, microcracks starts to localize and creates a major crack. This major crack is the part of fracture process zone. They also give some results about the effect on fracture process zone due to size of specimen and aggregates.

1. The size of the fracture process zone increases as there is an increase in size of specimen and also it has been noticed that the increasing rate was not in proportion with the size of specimen.
2. It has been depicted that growth rate of fracture process zone width was smaller than that of the specimen.
3. Increasing rate of fracture process zone length was way larger than that of the specimen size.
4. Ligament length also affects the dimension of fracture process zone.
5. It has been observed that in case of short ligament length, fracture process zone does not develop completely but in case of middle and large ligament length such problem does not occur.

6. Width of the fracture process zone increases but the length of fracture process zone decreases with the increase in size of the aggregate as shown in Figure 2.1 below:

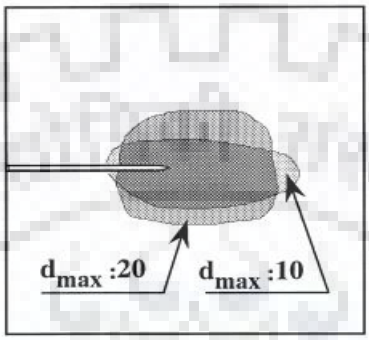

Figure 2.1: Comparision of FPZ with different aggregate. [3]

Yao et al. [4] explained about the mechanism of development of fracture process zone in concrete. As it has been clear that principle of linear elastic fracture mechanics cannot be applied on concrete and the existing models are not giving satisfactory results about fracture process zone. The authors have proposed a new model called "banding microcrack model" for finding innate characteristic and size of fracture process zone.

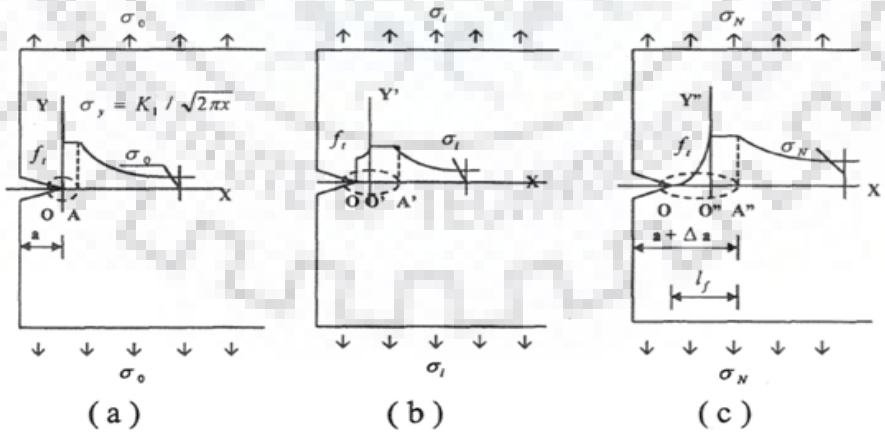

Figure 2.2: Schematic illustration of banding microcrack model. [4]

The model proposed by Yao et al. is illustrated in Figure 2.2. With the increase in load, microcracks starts to grow near the crack tip. Portion between *O'* to *A'* is called microcracks

creation zone and portion between *O* to *O'* is called microcrack extension zone. Because of softening, cohesive stress reduces in microcrack extension zone. When stress reaches failure stress, tip of crack moves to point *O"* and stress at *O* will become zero. Therefore, length between tip of crack and *A"* can be called as FPZ.

Wei et al. [5] have developed a numerical approach to understand and investigate the evolution of crack growth. In this method, initial fracture toughness [K_{ini}] has been used to develop a crack propagation criterion. The effects on evolution of FPZ length (l_{FPZ}) because of various conditions are studied based on numerical analysis results. The significance of K_R-curve has been studied based on the numerical approach adopted. Initial fracture toughness is the main index for estimating crack initiation and crack propagation criterion proposed in this paper and it is described as follows:

$K_{PI} + K_{rI} < K_{ini}$, crack does not propagate,

$K_{PI} + K_{rI} = K_{ini}$, crack is in the critical state,

$K_{PI} + K_{rI} > K_{ini}$, crack propagate.

Here,

K_{ini}, = initial fracture toughness of concrete,

K_{PI} = stress intensity factor due to applied load,

K_{rI} = stress intensity factor due to cohesive stress.

Shah et al. [2] have studied notched beams subjected to quasi-static cyclic and fatigue loading tested in 3-point bending configuration with continuous crack mouth opening displacement monitoring. Crack growth under constant amplitude fatigue loading comprises two phases: transient phase (deceleration phase) and steady state phase (acceleration phase). The crack length where crack growth rate changes from deceleration to acceleration corresponds peak load response of quasi static loading.

Xu et al. [6] have developed a numerical approach for determination of crack extension resistance [K_R]curve. The variation in the fracture process zone (FPZ) in concrete is taken in to consideration for the evaluation of K_R curve. The authors have used linear asymptotic superposition assumption **[7]** for the calculation of FPZ. The fracture zone has been split in to 3 stages. These stages are explained in the terms of cohesive or tensile stress, which has been distributed in FPZ. The K_R values has been calculated by using the fracture resistance (caused

by cohesive stress) and initial fracture toughness. The K_R curve of the beam is initially increasing and then it became constant when the fracture process zone is fully developed.

Chatti et al. [8] have stated that fatigue crack propagation is a nonlinear phenomenon. According to the authors, crack growth consists of two stages, namely, transient stage or deceleration stage and second is steady state stage or acceleration stage. A new approach has been introduced by the authors in which fatigue crack resistance has been calculated by using stress intensity and crack growth rate. It has been concluded that the shape of crack extension resistance in static loading is same as in fatigue loading but the value of fatigue crack resistance is lower than the static one.

Ruiz et al. [9] have developed a cohesive model to study the fracture process zone. Here fracture process zone is presented as a material parameter. Authors have defined a new characteristic length based on tensile and compressive strength which is approximately equivalent to fully developed fracture process zone. The cohesive model adopted is verified against various experimental results.

CHAPTER 3

METHODOLOGY

In this study, an attempt has been made to characterize the fracture process zone analytically using the available experimental results [10]. Bhowmik & Ray [10] have performed experiments on concrete beams under static and fatigue loading cases. In their study, geometrically similar beam specimens of three different sizes, casted from ordinary portland cement (OPC), have been considered for the experimental study and determination of various fracture parameters such as stress intensity factor (SIF), crack extension resistance and fracture process zone (FPZ). The specimen sizes were decided as per the recommendation given by the RILEM technical committee 89-FMT. The maximum size of the coarse aggregates used in concrete was 12.5 mm. The beam specimens were tested after 28 days to determine the concrete strength parameters. The characteristic strength (f_{ck}) of concrete was found to be 33.68 MPa. The modulus of elasticity (E_c) and tensile strength(f_t) are measured from empirical formulas and are determined as 29000 MPa and 4.06 MPa respectively. The geometrical details of beam specimen considered in this experiment are in Table 3.1. The notch length here is denoted as a_o.

Table 3.1: Beam dimensions for different specimens [10]

Specimen Name	**Overall Length (*L*) mm**	**Loading Span (*S*) mm**	**Width (*B*) mm**	**Depth (*D*) mm**	**(a_o/D)**	**(S/D)**
Small	300	200	50	50	0.2	4
Medium	550	400	50	100	0.2	4
Large	1000	800	50	200	0.2	4

The notch length to beam depth ratio was considered as 0.2 for all the specimens. The notch was provided along the central axis in the transverse direction, to ensure that the crack propagates through the center of the beam in the vertical direction.

3.1. Static test procedure

The TPB test under static loading was carried out by Bhowmik & Ray [10]. The above specimens were tested till the ultimate damage of the specimen. The cracking pattern of all specimen was observed and it was found that the crack line had followed the ligament center line as desired. Thus, the failure mode of every beam was geometrically similar. The load-CMOD curve for each beam specimen obtained have been documented below in Figures below:

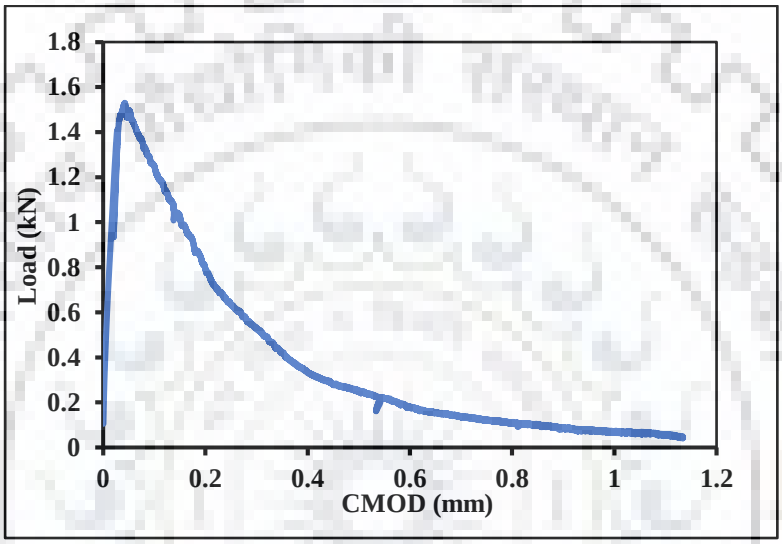

Figure 3.1: Load vs CMOD for small specimen [10]

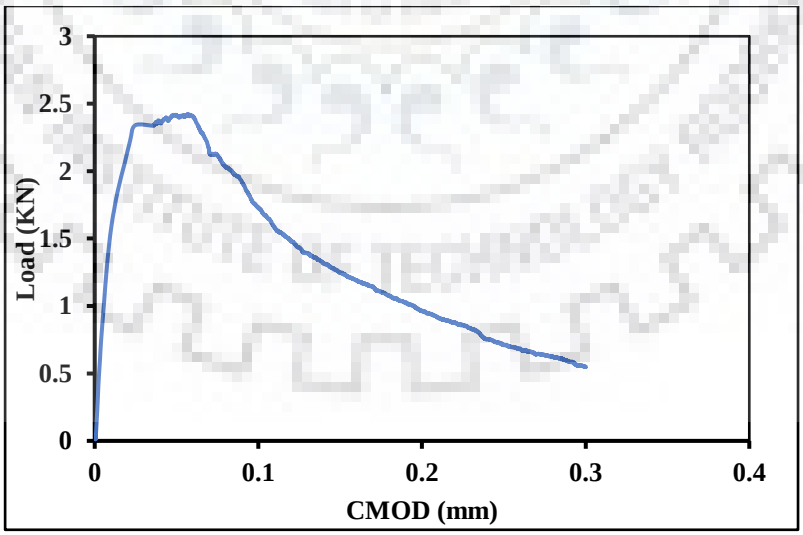

Figure 3.2: Load vs CMOD for medium specimen [10]

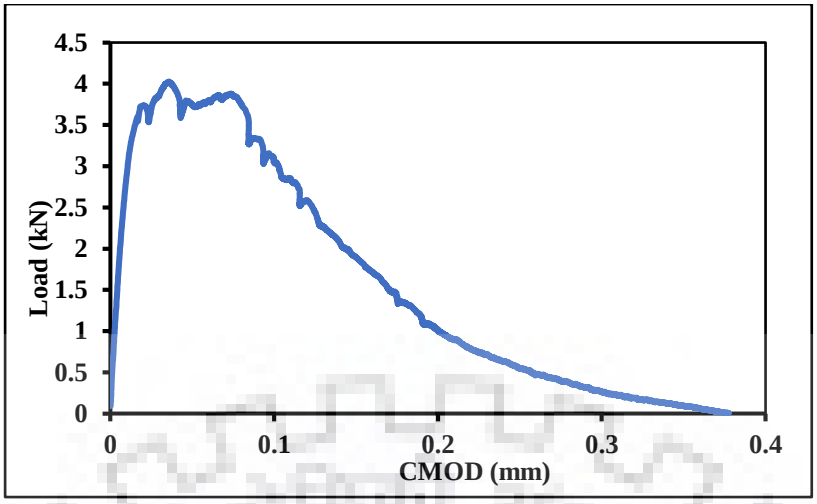

Figure 3.3: Load vs CMOD for large specimen [10]

For small, medium and large specimens, the peak load values were found as 1.53 kN, 2.42 kN and 4.02 kN respectively. The peak load values of specimen are increasing with the size of specimen. After peak load a gradual softening of the curve was observed which indicates the quasi-brittle nature of the concrete. In this thesis, the experimental results have been used to evaluate the various fracture parameters as discussed below.

3.2. Important fracture parameters

3.2.1 Effective crack length (*a*):

In order to calculate effective crack length, Xu and Reinhardt [7] proposed a linear asymptotic superposition assumption. In this approach, the specimen is loaded and unloaded in cyclic manner and the nonlinear behaviour of concrete and its residual deformation were taken into consideration approximately. Thus, linear elastic fracture mechanics (LEFM) becomes a good enough approximation to judiciously describe the fracture process zone. According to principles of linear elastic fracture mechanics (LEFM), the crack length (a) values can be calculated by the following Equation [6]:

$$CMOD = \frac{24P}{EB}\lambda\left[0.76 - 2.28\lambda + 3.87\lambda^2 - 2.04\lambda^3 + \frac{0.66}{(1-\lambda)^2}\right] \quad \ldots \text{Eq. (1)}$$

Where,

CMOD = crack mouth opening displacement

$\lambda = (a+H_0)/(D+H_0)$

a = effective crack length

D =depth of the tested beam

H_0 = thickness of knife edge (1.17mm)

B = thickness of the tested beam

E = Young's modulus of concrete

P = applied load.

3.2.2. Cohesive stress (σ):

As fracture process zone increases, cohesive stress within the fracture process zone decreases. Reinhardt et al. **[6]** proposed an empirical formula to calculate cohesive stress as per traction separation law of concrete.

$$\sigma(w) = f_t \left\{ [1 + (c_1 w/w_o)^3] e^{-\frac{c_2 w}{w_o}} - (w/w_o)(1 + c_1{}^3) e^{-c_2} \right\}$$

...Eq. (2)

Where,

f_t = tensile strength of concrete.

w = crack opening displacement.

w_o = stress-free crack opening displacement.

c_1, c_2 are material parameters

The values of c_1, c_2 and w_o are taken as 3, 7, and 0.16 mm respectively, for any normal concrete.

3.2.3 Crack opening displacement (*w*):

As can be seen that the cohesive stress is a function of crack opening displacement (*w),* it becomes vital to calculate crack opening displacement (*w).* Acc. to Jenq and shah **[11]** crack opening displacement (*w)* can be calculated as

$$w(x) = CMOD\sqrt{(1 - x/a)^2 + (1.081 - 1.149a/D)[x/a - (x/a)^2]}$$

…Eq. (3)

Where,

CMOD = crack mouth opening displacement.

a = effective crack length.

D = depth of beam.

x = distance from the crack mouth.

3.2.4. Fracture process zone (l_{fpz}):

Fracture process zone is the intermediate space between cracked and un-cracked portion. As the crack propagates, the fracture process zone also starts to increase. FPZ consist of micro cracks situated near crack tip. Therefore, this act as a bridging zone between cracked and un-cracked area. Equations 2 and 3 can be used to calculate the fracture process zone. FPZ can also be calculated by using the concept of fracture energy.

3.2.5 Specific fracture energy (G_F):

The specific fracture energy or the energy release rate is the rate at which material releases energy as it undergoes fracture. Fictitious crack model is proposed by Hillerborg [1] for concrete fracture and can be used to calculate fracture energy. The following Equation is used for the calculation of fracture energy.

$$G_F = \frac{1}{B.(D - a_o)} \int P.d\rho$$

…Eq. (4)

Where,

a_o = initial notch or crack length.

D = Specimen width in the crack growth direction.

B = specimen thickness.

P = vertical displacement.

ρ = displacement.

3.2.6. Characteristic length (l_{ch}):

The fracture process zone length is related with many characteristic lengths. Characteristic length is the material property and is comparable to the size of FPZ based on fictitious crack model. The expression for characteristic length as given by hillerborg is [9]:

$$l_{ch} = \frac{G_F.E_c}{f_t^{\,2}}$$

…Eq. (5)

Where,

G_F = Fracture energy.

f_t = Tensile strength of concrete.

E_c = Young's modulus of elasticity of concrete

3.2.7 The length scale (l_s):

Since fracture can occur under both tensile and compressive stresses, the characteristics length is generally defined separately for both cases. Ruiz et al. [9] proposed an intermediate length scale which includes the effect of both tensile and compressive fracture for a 3-point bending test as presented below.

$$l_s = \frac{G_F . E_c}{f_t . f_c}$$

…Eq. (6)

Where,

G_F = fracture energy.

f_t = tensile strength of concrete.

E_c = young's modulus of elasticity of concrete

f_c = compressive strength.

3.2.8 Fracture process zone (l_{fpz}):

Length of fracture process zone (l_{fpz}) can be defined in terms of length scale (l_s) as provided below [9].

$$l_{fpz} = \frac{w_{cr}}{w_{cr1}} l_s$$

…Eq. (7)

Where,

w_{cr} = critical crack opening as per linear cohesive law.

w_{cr1} = critical crack opening as per bi-linear cohesive law.

l_s = the length scale.

3.2.9. Determination of crack extension resistance (K_R) curve [6]:

Crack extension resistance of concrete depends upon two factors. One is the initiation toughness K_{ini} and the other is the cohesive toughness K_σ.

Initiation toughness (K_{ini}):

The initiation toughness is the property of the material. It is the intrinsic material resistance offered against crack propagation. Crack propagation initiates in a structure when the stress intensity factor caused by the loads applied exceed the initiation toughness.

Cohesive toughness (K_σ):

The cohesive toughness is a function of the length of FPZ, concrete's tensile strength and distribution of cohesive stress in the FPZ. According to Reinhardt and Xu [9], K_R can be represented as:

$$K_R(\Delta a) = K_{ini} + K_\sigma \quad \ldots(8)$$

Where, $\Delta a = a - a_o$, crack length extension.

The entire fracture process in concrete is divided into three stages to measure the crack extension resistance.

Stage I: When $a = a_o$

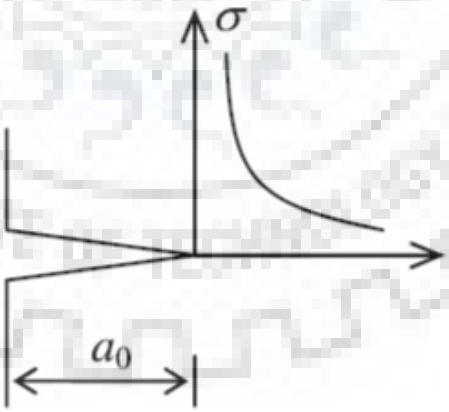

Figure 3.4: Cohesive stress distribution at $a = a_o$ [6]

During this stage, no crack extends beyond the notch that was initially provided in the specimen. Thus, no cohesive stress is encountered and the crack extension resistance becomes equal to initiation toughness

$K_R = K_{ini}$ for $a = a_o$

Stage II: when $a_o < a < a_{wo}$

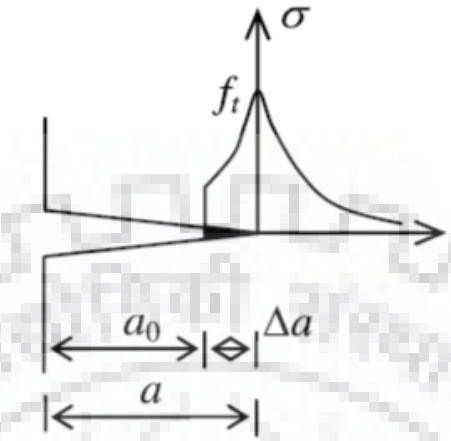

Figure 3.5: Cohesive stress distribution at $a_o < a < a_{wo}$ [6]

Here, a_{wo} = effective crack length when $CTOD = w_o$

When the load applied on the specimen increases, a stage is reached when the crack starts to propagate. This implies that the fracture process zone progresses and cohesive stress starts to act within the FPZ. Thus, the crack extension resistance becomes larger than K_{ini}.

Stage III: when $a > a_{wo}$

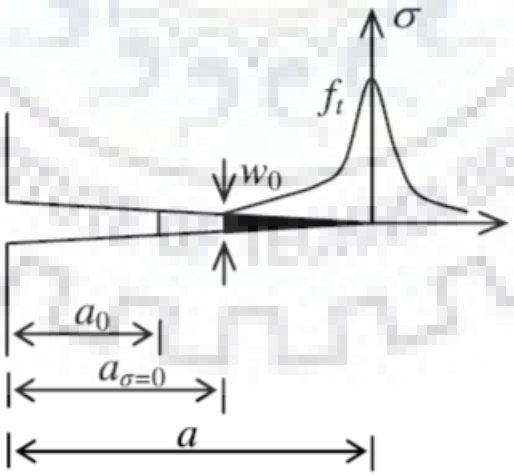

Figure 3.6: Cohesive stress distribution at $a > a_{wo}$ [6]

When *CTOD* exceeds w_o, the cohesive stress at the notch tip becomes zero. At this stage, it has been observed that FPZ is completely developed and the traction free crack propagates further as the FPZ shifts with varying length.

To determine K_R curve, the value of K_{ini} is required, the external load that is applied on the three-point bending (TPB) test, when it reaches the initial cracking load (P_{ini}), the effective crack length becomes equal to notch length a_o. The concrete is considered to be elastic till this point and the principles of LEFM can be applied for the calculation of K_{ini}. The formula for K_{ini} is provided below [6].

$$\boldsymbol{K = \frac{3PL\sqrt{a}F_2(a/D)}{2BD^2}} \quad \text{…Eq. (9)}$$

Where,

$$\boldsymbol{F_2\left(\frac{a}{D}\right) = \frac{1.99-\left(\frac{a}{D}\right)*\left(1-\frac{a}{D}\right)*[2.15-3.93*a/D+2.7*(a/D)^2]}{\left(1+\frac{2a}{D}\right)*(1-a/D)^{1.5}}} \quad \text{…Eq. (10)}$$

Since, it is very difficult to find out P_{ini} through laboratory tests, Xu and Reinhardt [6] proposed an alternative approach for calculating K_{ini}. Specimens are loaded up to P_{max}, where the concrete reaches the critical stage and this is the stage between stable and unstable crack propagation. At this stage, concrete is still in the elastic stage, LEFM principle can be applied to find the stress intensity factor. At this point $P=P_{max}$, $CMOD = CMOD_c$, $a = a_c$ and stress intensity factor (K) calculated using LEFM and crack extension resistance (K_R) are considered to be equal.

Thus, we can find K_{ini} using relation provided below [6]:

$$\boldsymbol{K_{ini} = K - K_\sigma} \quad \text{…Eq.(11)}$$

Where K_σ can be obtained from following Equation [6]:

$$K_\sigma = \int_{a_o}^{a} \frac{2\sigma F_1\left(\frac{x}{a}, \frac{a}{D}\right)}{\sqrt{\pi a}} dx$$

…Eq. (12)

$$F_1 = \frac{3.52(1-x/a)}{(1-a/D)^{1.5}} - \frac{4.35-\frac{5.28x}{a}}{\left(1-\frac{a}{D}\right)^{0.5}} + \left[\frac{1.3-0.3\left(\frac{x}{a}\right)^{1.5}}{\sqrt{1-\left(\frac{x}{a}\right)^2}} + 0.83 - \frac{1.76x}{a}\right] * \left[1-(1-x/a)a/D\right]$$

…Eq. (13)

Knowing K_{ini}, we can easily determine the K_R curve using the Equation provided below [6]:

$$K_R = K^{ini} + \int_{a_o}^{a} \frac{2\sigma F_1\left(\frac{x}{a}, \frac{a}{D}\right)}{\sqrt{\pi a}} dx$$

…Eq. (14)

Where,

σ = Bridging stress

a = crack length

D = Depth of beam

x = Distance from notch tip

3.3. Fatigue test procedure:

In this experimental work by Bhowmik & Ray [10] they have carried out the TBP test under fatigue loading. In fatigue testing, repetitive load cycles are applied on concrete specimen until complete failure. During the entire test run, the loads, counts, time, stroke and CMOD are recorded for each cycle. The minimum load (P_{min}) and maximum load (P_{max}) for first 200 cycles was taken as 0.1 kN and 0.5 kN. After every 200 cycles of load, the P_{max} was increased by 500 N and CMOD was recorded for every loading and unloading cycles. The values of modulus of elasticity and tensile strength of concrete during the experiment was obtained as 29000 MPa and 4.06 MPa respectively. The load-CMOD plots for selected no. of cycles for small, medium and large beam specimen are shown in Figures below:

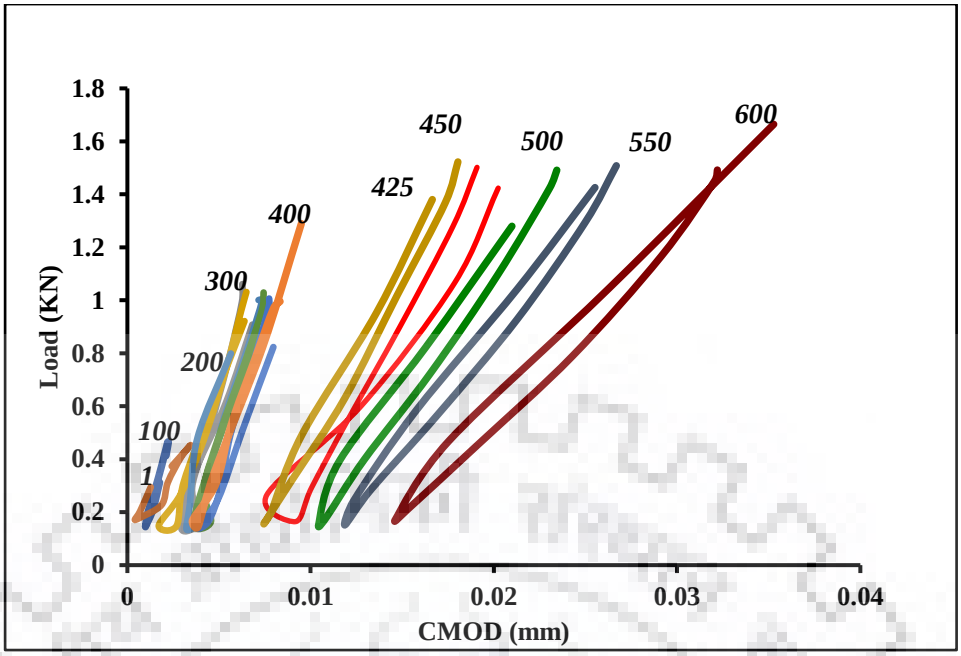

Figure 3.7: Load-CMOD plot for small beam specimen [10]

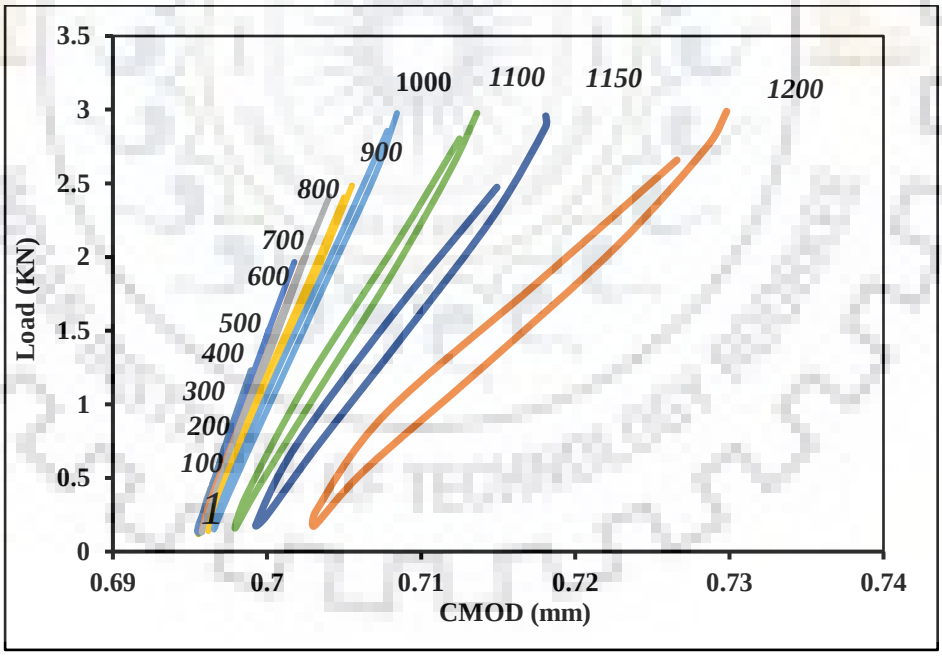

Figure 3.8: Load-CMOD plot for medium beam specimen [10]

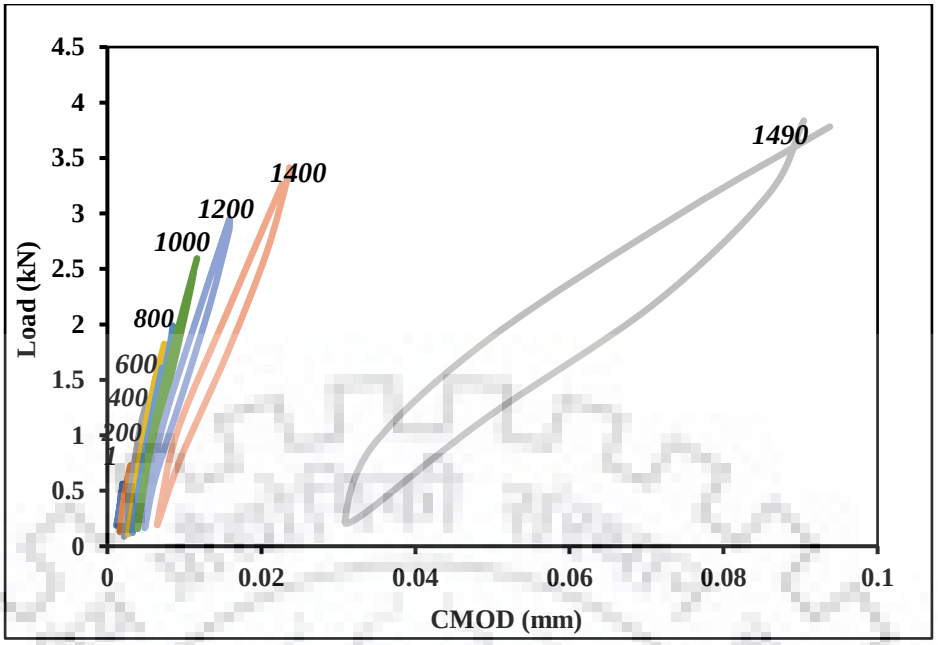

Figure 3.9: Load-CMOD plots large beam specimen [10]

The discussed experimental results [10] have been used in this study to obtain various fracture parameters. A compliance calibration equation for small, medium and large size beam specimen has been obtained. Compliance calculation from load – CMOD curve of different specimens has been carried out for each cycle. Calculation of (a_o/D) and crack length from compliance calibration equation was done for each cycle. Thereafter, crack growth rate (da/dN) values have been obtained with respect to stress intensity factor (ΔK). The values obtained have been used to plot the logarithmic variation of crack growth rate and stress intensity factor to determine the Paris law constant from linear regression. The equation for Paris law is given below [8].

$$\frac{da}{dN} = C(\Delta K)^m \quad \text{…Eq. (15)}$$

Where,

C and m are Paris law constants.

Now, in order to determine the crack extension resistance, an approach proposed by Reinhardt and Xu [6] is adopted and it is given below:

$$K_R\,(\Delta a) = K_{ini} + K_\sigma \qquad \text{…Eq.(16)}$$

Here,

K_R = Crack extension resistance of the beam.

K_{ini} = Fracture toughness of beam.

K_σ = Resistance due to cohesive stress and is given below:

$$K_\sigma = \int_{a_o}^{a} \frac{2\sigma F_1\left(\frac{x}{a},\frac{a}{D}\right)}{\sqrt{\pi a}}\,dx \qquad \text{…Eq. (17)}$$

Where,

$$F_1 = \frac{3.52(1-x/a)}{(1-a/D)^{1.5}} - \frac{4.35-\frac{5.28x}{a}}{\left(1-\frac{a}{D}\right)^{0.5}} + \left[\frac{1.3-0.3\left(\frac{x}{a}\right)^{1.5}}{\sqrt{1-\left(\frac{x}{a}\right)^2}} + 0.83 - \frac{1.76x}{a}\right]*\left[1-(1-x/a)a/D\right] \qquad \text{…Eq. (18)}$$

σ = Bridging stress

a = crack length

D = Depth of beam

x = Distance from notch tip

The initial fracture toughness has been taken as same as obtained in static loading and cohesive toughness has to be calculated at each loading cycle.

CHAPTER 4
WORK DONE

4.1. Static test calculations

Under the static load test for small, medium and large specimens, the peak load values were found to be 1.53 kN, 2.42kN and 4.02kN respectively [10]. After peak load, a gradual softening behavior is observed which represents the quasi-brittle nature of the concrete. A crack initiation was seen at 95% of the peak load.

The following important fracture parameters are calculated using the methodology discussed in chapter 3. Experimental results of Bhowmik & Ray [10] are used for this study.

4.1.1 Effective crack length (*a*):

This is the sum of initial notch (a_o) and crack extension when the crack propagates. The crack length values are calculated by using Equation 1. The effective crack length at peak load is called critical crack length and the calculated values are presented in Table 4.1.

Table 4.1: Critical crack length values

S. No.	Specimen	Peak load (kN)	Critical crack length (a_c) (mm)	a_c/D
1	Small	1.53	26.38	0.52
2	Medium	2.42	44.63	0.44
3	Large	4.02	68.75	0.34

4.1.2 Crack opening displacement (*w*):

As the crack propagates in the beam, crack width increases and there is decrease in cohesive stress ahead of the crack tip. A stage comes when the value of cohesive stress at the crack tip becomes zero. The crack width at which cohesive stress becomes zero at crack tip has been taken as 0.16 [6]. The critical crack opening displacements at peak load are shown in Table 4.2. below.

Table 4.2: Crack opening displacement values

S. No.	Specimen	Peak load (kN)	w_c (mm)	a_c/D
1	Small	1.53	0.029	0.52
2	Medium	2.42	0.038	0.44
3	Large	4.02	0.021	0.34

4.1.3. Fracture process zone (l_{fpz}):

Fracture process zone is the intermediate space between cracked and uncracked portion. With the propagation of crack, the fracture process zone also starts to increase. FPZ is the zone of extensive microcracking and situated ahead of crack tip. Therefore, FPZ acts as a bridging zone between cracked and uncracked area. Fracture process zone calculated for different specimen are shown in Table 4.3. below.

Table 4.3: FPZ values

S. No.	Specimen	Peak load (kN)	l_{fpz} (mm) (critical)	l_{fpz} (mm) (fully developed)
1	Small	1.53	16.38	30.71
2	Medium	2.42	24.63	59.85
3	Large	4.02	28.75	120.47

Further, development and propagation of fracture process zone as a function of relative crack depth is shown in Figures 4.1, 4.2 and 4.3 for small, medium and large beam respectively.

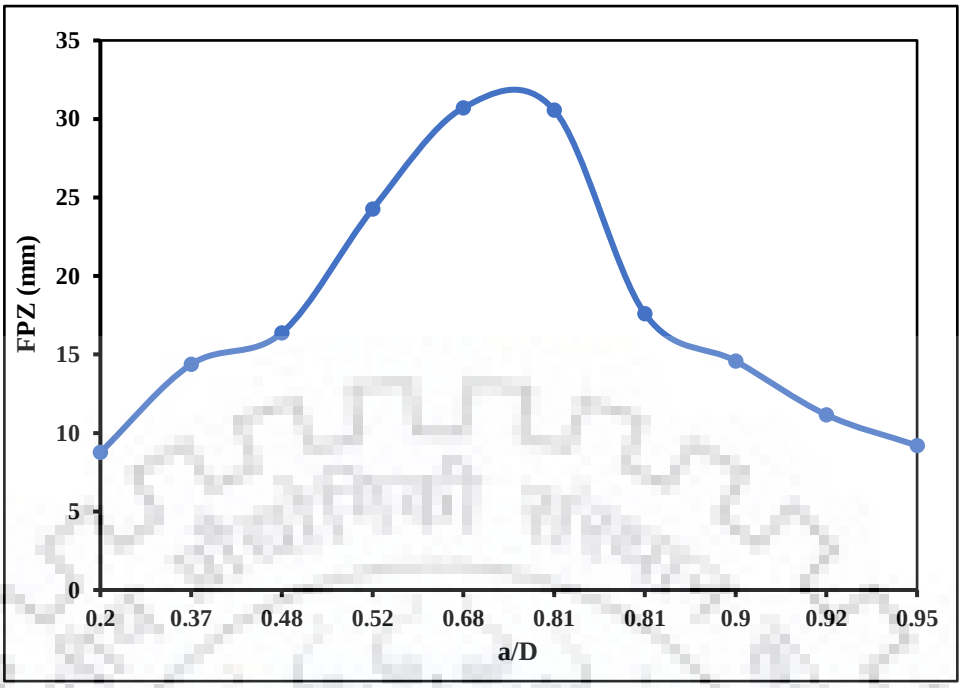

Figure 4.1: Variation of FPZ in small specimen

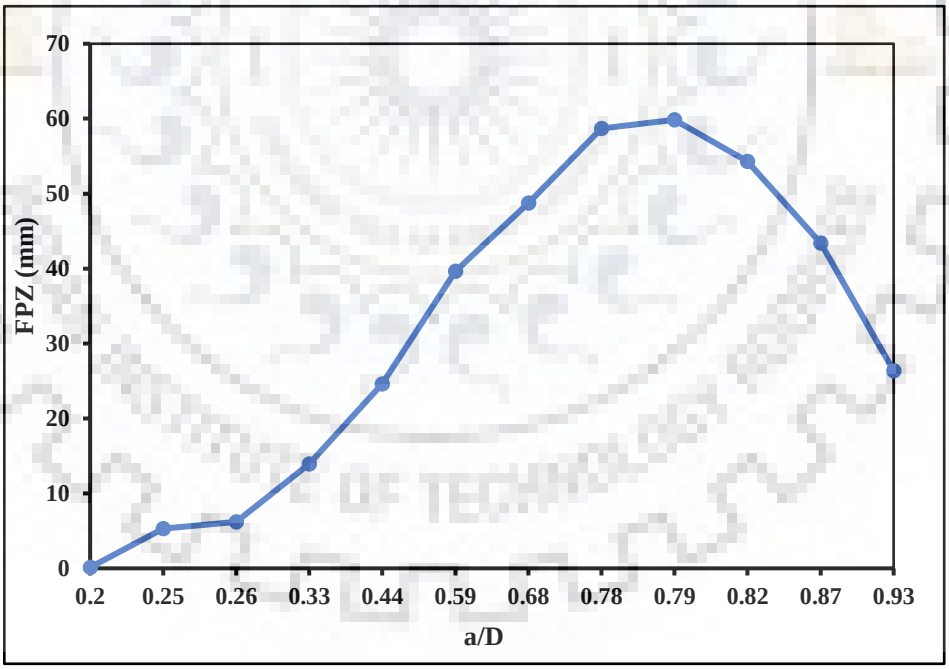

Figure 4.2: Variation of FPZ in medium specimen

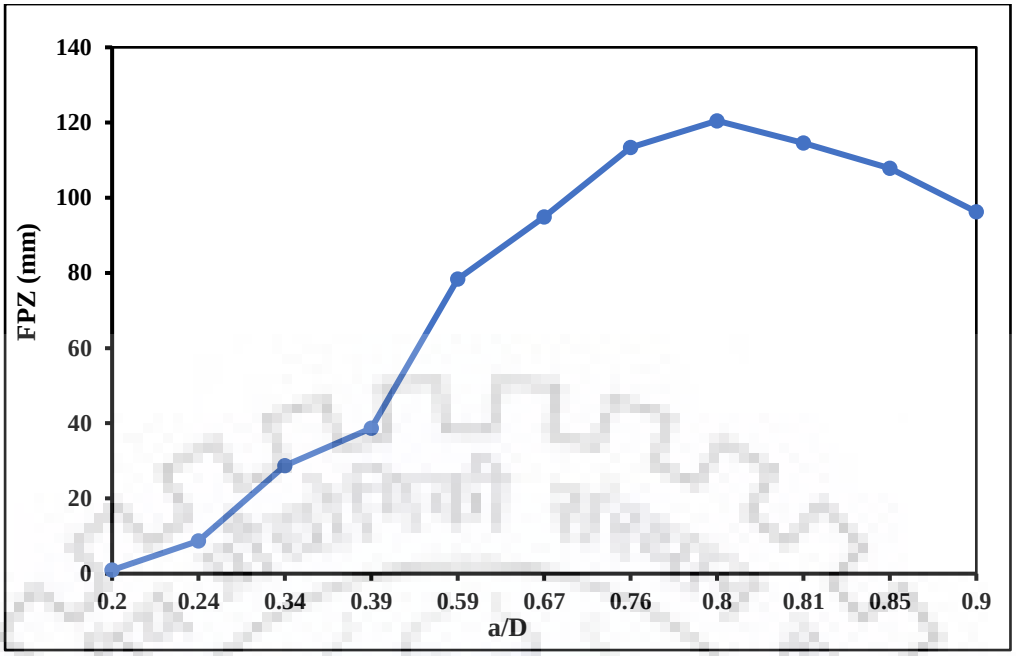

Figure 4.3: Variation of FPZ in large specimen

It may be observed that in all specimen, up to a relative crack depth about a/D = 0.8, fracture process zone increases and attains its maximum value and thereafter starts to decrease. Such reduction is due to the fact that at that point CTOD exceeds w_o. w_o is that crack tip opening displacement at which stress at crack tip becomes zero. A traction free zone is developed in front of the tip of notch. With further increase of the CTOD, the new stress-free crack propagation occurs and the FPZ shifts with varying length and starts to decrease. It has been observed that fully developed FPZ length increases when we increase the size of specimen. So, it can be concluded that fracture process zone is size dependent.

4.1.4 Fracture energy (G_F):

Fracture energy for different specimen calculated using Equation 4 are presented in Table 4.4. below

Table 4.4: Fracture energy values

S. No.	Specimen	G_F (N/mm)
1	Small	0.2
2	Medium	0.221
3	Large	0.36

It has been observed that fracture energy is increasing with the specimen size which confirms the existence of size effect in concrete.

4.3.5 Characteristic length (l_{ch}):

The values of characteristic length are obtained by using Equation 5 as shown in Table 4.5 below:

Table 4.5: Characteristic length values

S. No.	Specimen	Characteristic length (mm)
1	Small	351.66
2	Medium	389.03
3	Large	632.98

The values of characteristic length are increasing with the specimen size, confirms the existence of size effect in concrete.

4.3.6 Length scale (l_s):

The length scale values are obtained by using Equation 6 as shown in Table 4.6 below:

Table 4.6: Length scale values

S. No.	Specimen	l_s (mm)
1	Small	42.4
2	Medium	46.89
3	Large	76.3

The length scale values are considered as an approximation to the size of FPZ. The length scale values obtained has been further used for estimation of fracture process zone. Fracture process zone (D_F) at peak load is given by [10]:

$$D_F = \frac{w}{w_{cr}} l_s$$

…Eq. 19

Where,

w = crack opening when cohesive stress at crack tip is half of tensile strength.

w_{cr} = crack opening when cohesive stress at crack tip is zero.

Using the above formula, fracture process zone at peak load was found to be 18 mm, 22.62 mm and 37.6 mm for small, medium and large specimen respectively and fully developed fracture process zone values are 84.3 mm and 137.4 mm for medium and large specimens. It was noted that the fracture process zone could not fully develop for small specimens because of small ligament size.

4.1.7. Comparison of fracture process zone

The FPZ length values are both evaluated by using linear asymptotic superposition assumption [9] in section 4.1.3 and method given by Ruiz [9] in section 4.1.6. The comparison of the values obtained for both critical and fully developed fracture process zone is shown in Table 4.7.

Table 4.7: Comparison of FPZ

S. no.	Specimen	Critical FPZ		Fully developed FPZ		
		Linear asymptotic superposition (mm)	Cohesive model (mm)	Linear asymptotic superposition (mm)	Cohesive model (mm)	Experimental results. [10]
1	Small	16.38	18	30.71	***	30.51
2	Medium	24.63	22.6	59.85	84.3	45.22
3	Large	28.75	37.6	120.47	137.4	101.28

The FPZ values are calculated at both the critical and fully developed stage. As we can see, the results obtained from linear asymptotic superposition assumption model are more reliable. Also, these values are compared to the results obtained by Bhowmik & Ray [10] which was 30.51 mm, 45.22 mm and 101.28 mm for small, medium and large specimen respectively as shown in Table 4.7.

4.1.8 Crack extension resistance (K_R):

The values of K_R at initial stage, at critical stage and at stress free notch tip has been calculated for each specimen and shown in Table 4.8 below.

Table 4. 8: K_R values of different specimen

S. No.	Specimen	a_o/D	K_{Rini} (MPa $m^{0.5}$)	a_c/D	K_{un} (MPa $m^{0.5}$)	a_{wo}/D	K_R (MPa $m^{0.5}$)
1	Small	0.2	2.221	0.52	2.39	0.81	2.6
2	Medium	0.2	1.1	0.44	1.9	0.79	2.5
3	Large	0.2	0.998	0.34	1.53	0.8	2.76

Variation of crack extension resistance with the relative depth have been shown in Figures 4.4, 4.5 and 4.6 for each specimen.

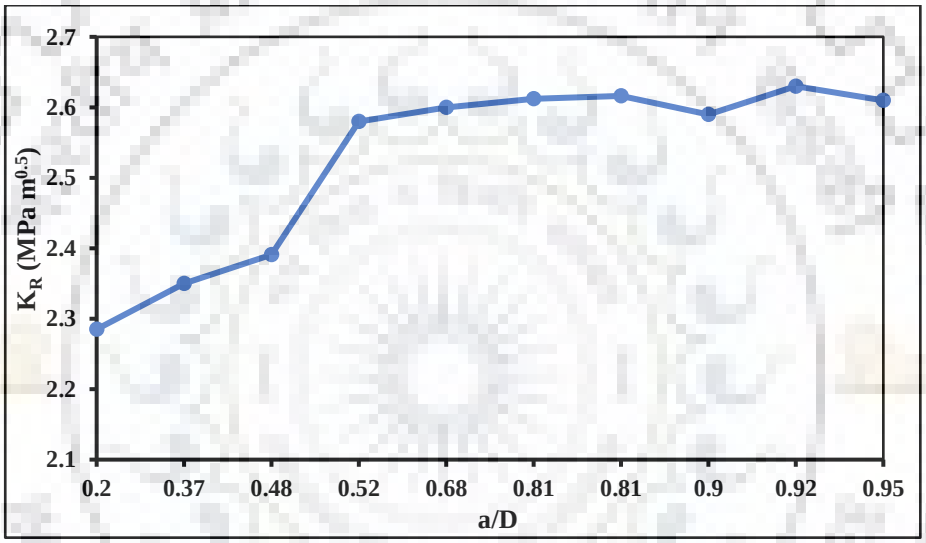

Figure 4.4: K_R values of small specimen

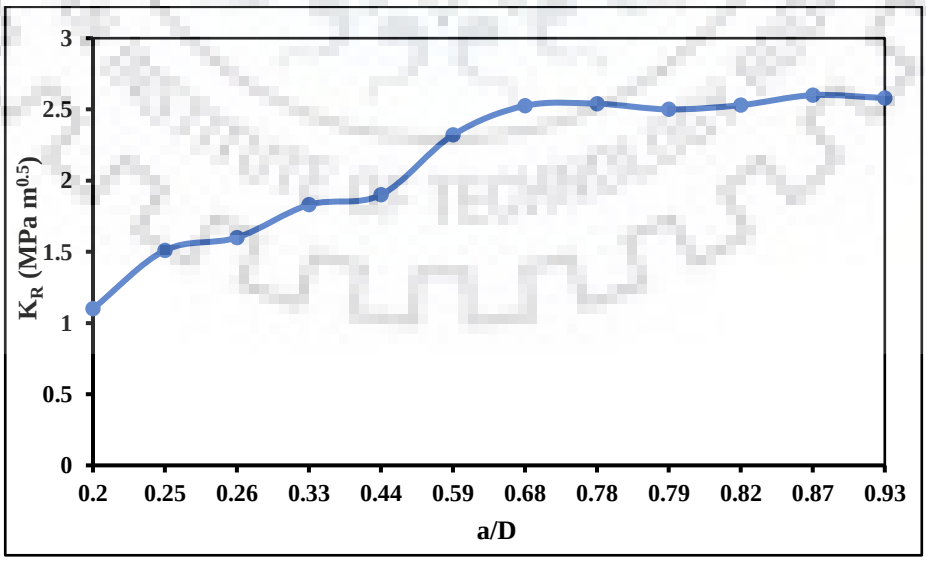

Figure 4. 5: K_R values of medium specimen

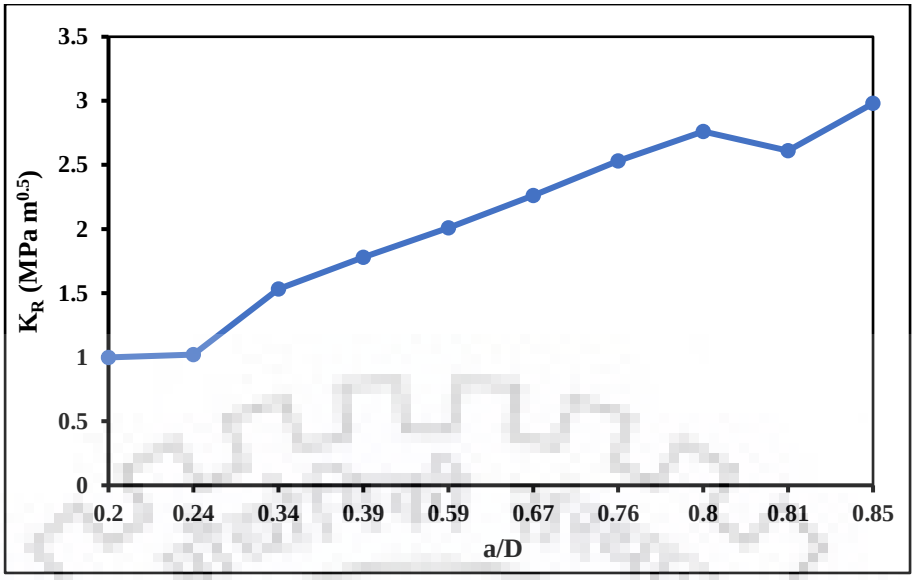

Figure 4. 6: K_R values of large specimen

It may be observed from the above plots that the crack extension resistance is independent of the specimen size. Crack extension resistance increases initially because of cohesive stress distribution within the fracture process zone. When fracture process zone attains its maximum at a/D = 0.8, cohesive stress reaches to zero at crack tip, Stress free surface starts to propagate. Crack extension resistance tends to constant after fracture process zone is fully developed because of propagation of stress-free surface as seen in the Figures 4.1, 4.2 and 4.3.

4.2 Fatigue test calculations:

The slope of load-CMOD plots obtained has been calculated by using the CMOD values in each cycle and as expected, gradual reduction has been seen in the slope of these curves with the increasing no. of loading cycles. Steady crack propagation is the main reason of this type of behavior. Figure 4.7. shows decrease in flexural stiffness with loading cycles and it is followed by rapid decrease in stiffness before failure. This behavior is similar for all specimen sizes considered and it has been concluded that specimen size does not influence rate of decrease of stiffness.

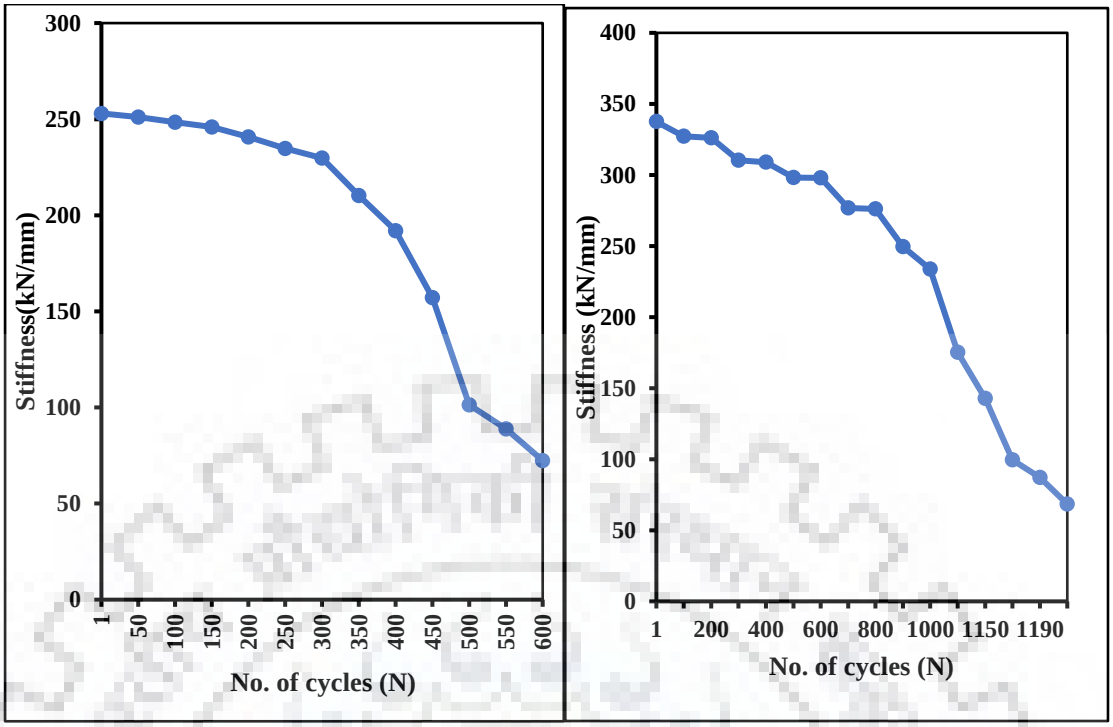

(a) (b)

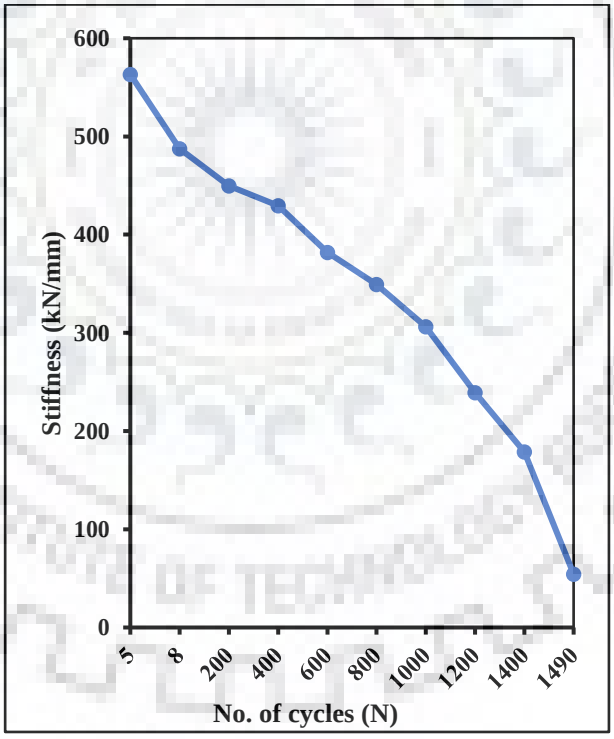

(c)

Figure 4.7: Stiffness-No of cycles (N) curve for small(a), medium(b) and large(c) specimens

By using the data from load-CMOD curve, CMOD compliance has been calculated from the slope of unloading portion. This CMOD compliance has been used to calculate the crack length. Since it is impossible to directly measure the crack length, a compliance calibration curve has generated for each size. The compliance calibration equation is given by: $y = 146104x^3 - 5244x^2 + 71.259x + 0.1055$, $y = 18263x^3 - 1311x^2 + 35.629x + 0.1055$ and $y = 1000000x^3 - 19021x^2 + 156.08x + 0.019$ for large, medium and small beam specimen respectively. The CMOD compliance has been calculated as the inverse of the slope of each cycle. This CMOD compliance has been used to calculate effective crack length in all three sizes. The calculated crack length has been shown in Figure 4.8.

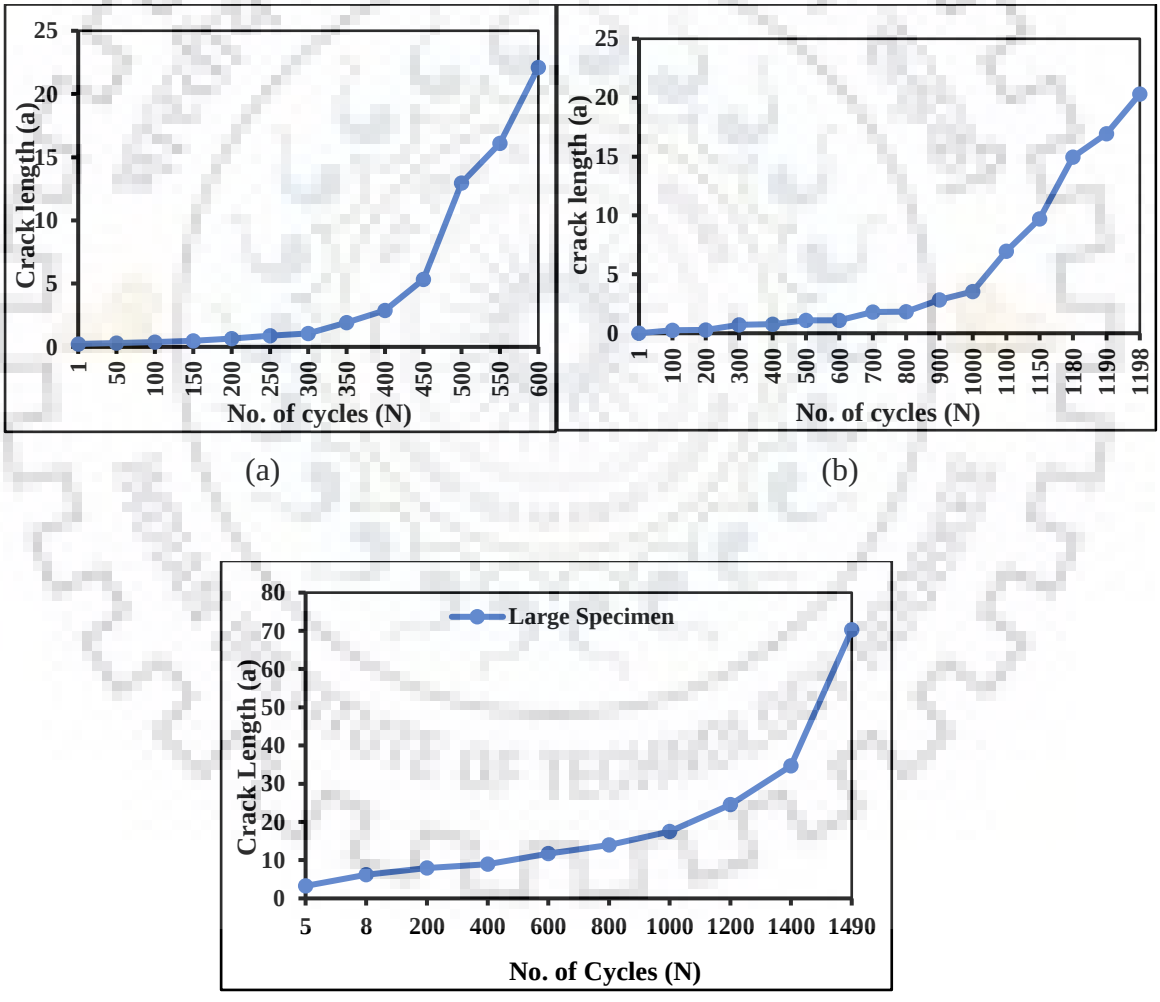

Figure 4.8: Crack length vs no. of cycles of small(a), medium(b) and large(c) beam specimen

Initially crack growth rate is very slow but, in the end, it accelerates rapidly in all three sizes. The crack growth rate for all three sizes with respect to crack length is shown in Figures 4.10,4.11 and 4.12 below:

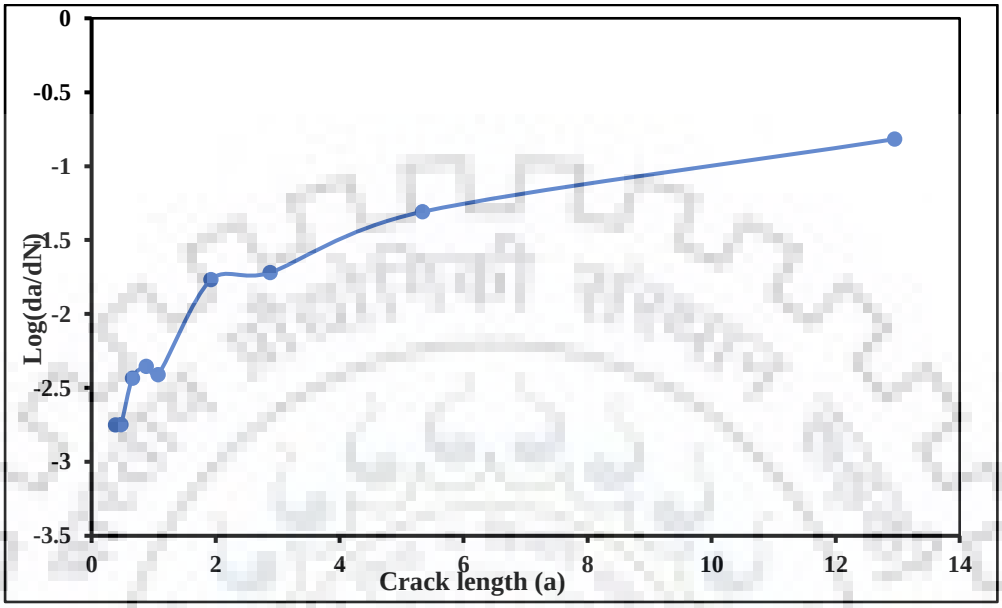

Figure 4.9: Crack growth rate in small specimen.

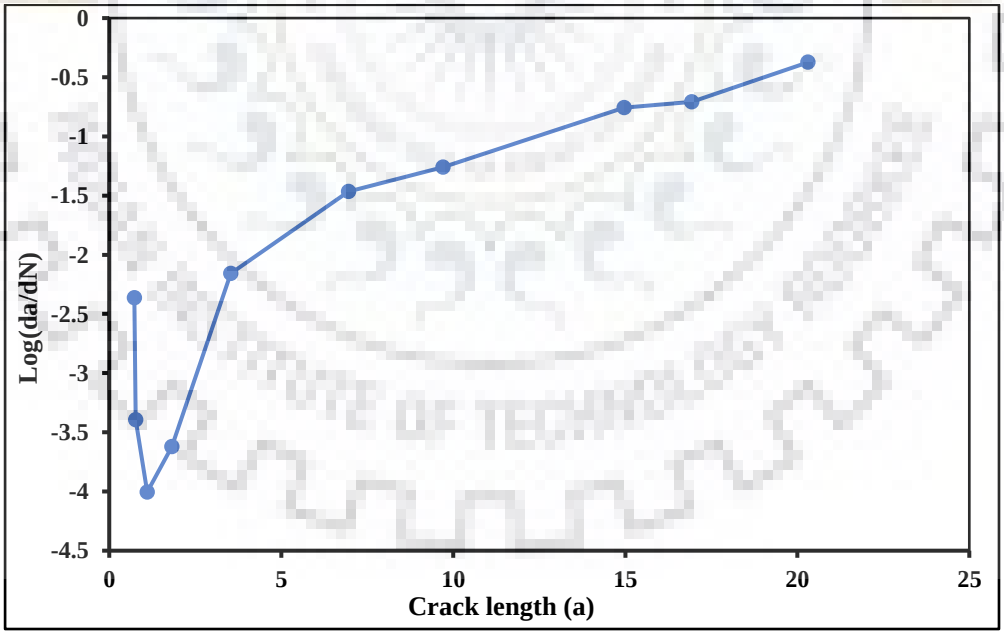

Figure 4.10: Crack growth rate in medium specimen.

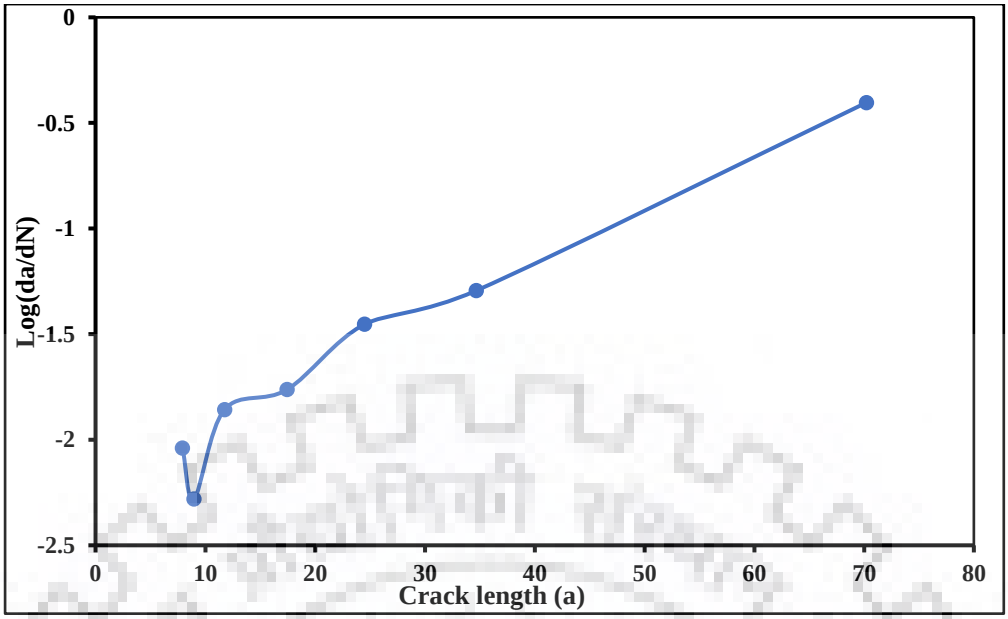

Figure 4.11: Crack growth rate in large specimen.

In the crack growth rate curves, two distinct stages are observed: a transient stage, in which crack growth rate is decreasing and a steady state stage where the rate is increasing. It has been observed that rate of crack growth has a deacceleration stage followed by an acceleration stage until failure.

Logarithmic variation of crack growth rate with stress intensity for small, medium and large beam specimen have been represented in Figures 4.12, 4.13 and 4.14 respectively. The *m* and *C* values has been calculated for each size using linear regression and shown in the Figures below.

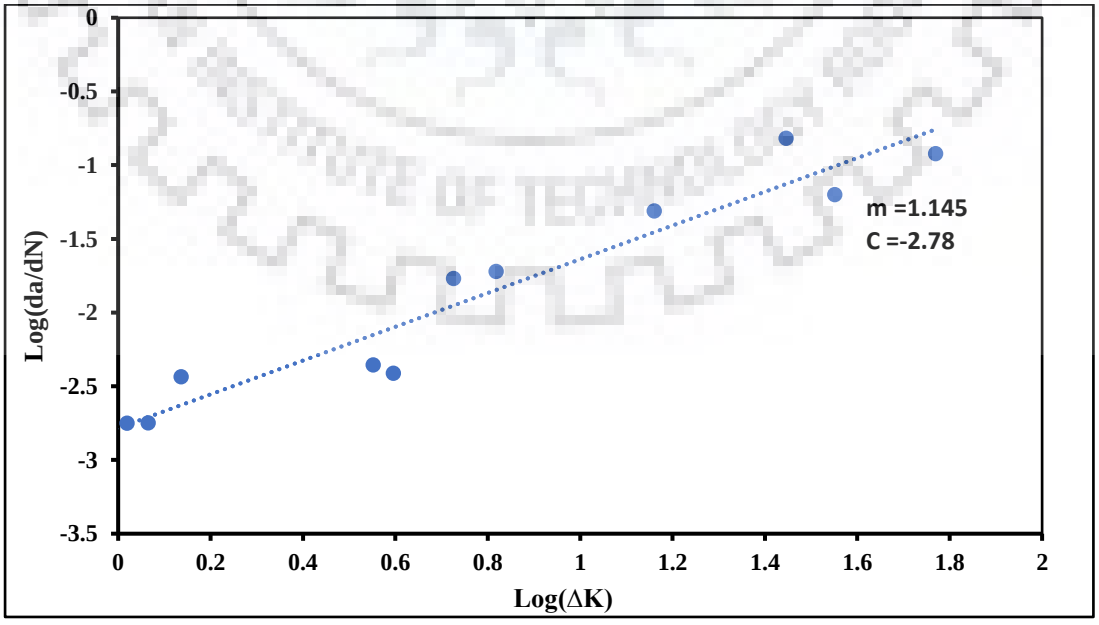

Figure 4.12: Linear regression plot for small specimen

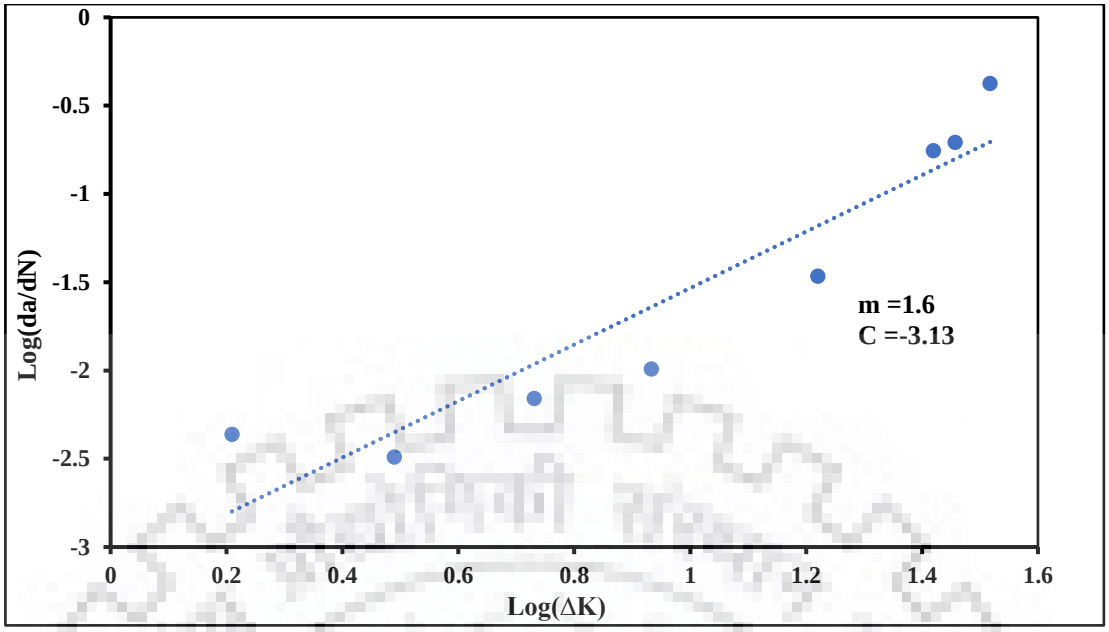

Figure 4.13: Linear regression plot for medium specimen

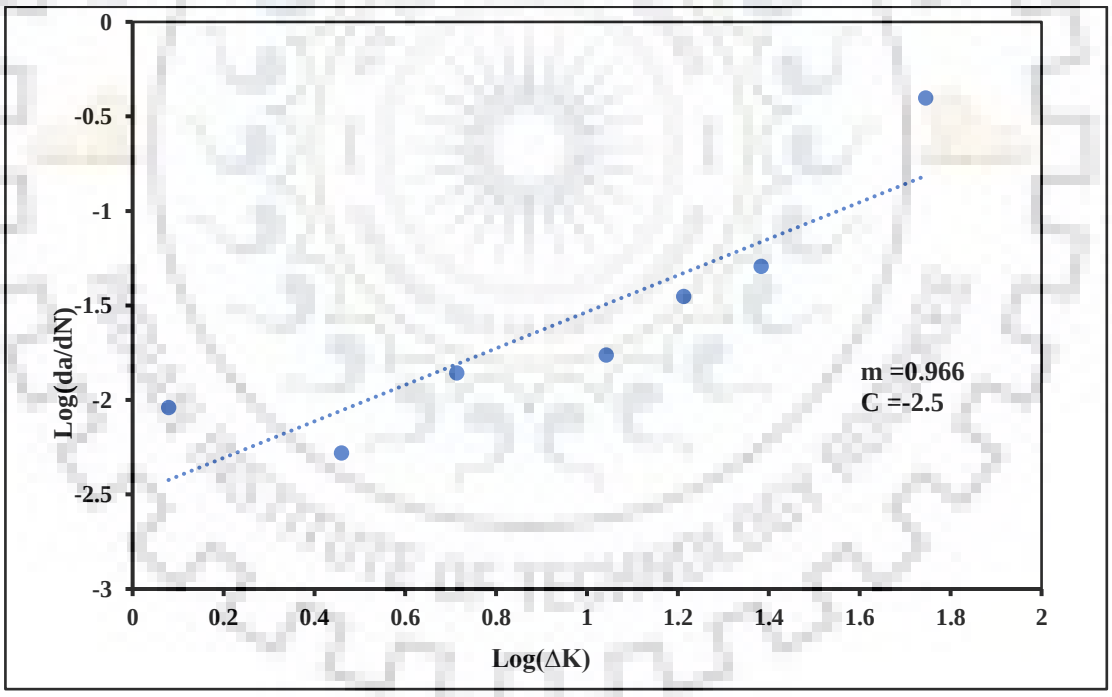

Figure 4.14: Linear regression plot for large specimen

The values of *m* and *C* are 1.145 and -2.78 for small, 1.6 and -3.13 for medium and 0.966 and -2.5 for large specimen. Here ΔK is the stress intensity factor range ($K_{max} - K_{min}$). The fatigue lifetime for small, medium and large specimen is recorded as 600, 1198 and 1490 respectively.

Now, to determine the crack extension resistance of all three-beam specimen, an approach given by Reinhardt and Xu [6] is adopted and it is given below:

$$K_R\,(\Delta a) = K_{ini} + K_\sigma \qquad \text{…Eq. (20)}$$

Here,

K_R = Crack extension resistance of the beam.

K_{ini} = Fracture toughness of beam.

K_σ = Resistance due to cohesive stress and is given below:

$$K_\sigma = \int_{a_o}^{a} \frac{2\sigma F_1\left(\frac{x}{a},\frac{a}{D}\right)}{\sqrt{\pi a}}\,dx \qquad \text{…Eq. (21)}$$

Where,

$$F_1 = \frac{3.52(1-x/a)}{(1-a/D)^{1.5}} - \frac{4.35-\frac{5.28x}{a}}{\left(1-\frac{a}{D}\right)^{0.5}} + \left[\frac{1.3-0.3\left(\frac{x}{a}\right)^{1.5}}{\sqrt{1-\left(\frac{x}{a}\right)^2}} + 0.83 - \frac{1.76x}{a}\right] * \left[1-(1-x/a)a/D\right] \qquad \text{…Eq. (22)}$$

σ = Bridging stress

a = crack length

D = Depth of beam

x = Distance from notch tip

According to Subramaniam et el. [2] fracture toughness (K_{ini}) of beam under fatigue loading can be considered as same as in static loading. therefore, the values of fracture toughness for small, medium and large beam is taken as 1.54, 0.946 and 0.769 respectively. To evaluate the resistance due to cohesive stress, crack opening displacement at which cohesive stress becomes zero at notch tip should be known. Crack opening displacement values at notch tip where stress decreases to zero are taken as 0.011 and 0.237 for medium and large beam specimen respectively [10]. For small specimen cohesive stress could not reaches to zero because of small ligament length.

Using the above equations, the crack extension resistance values are calculated and shown in Figures below:

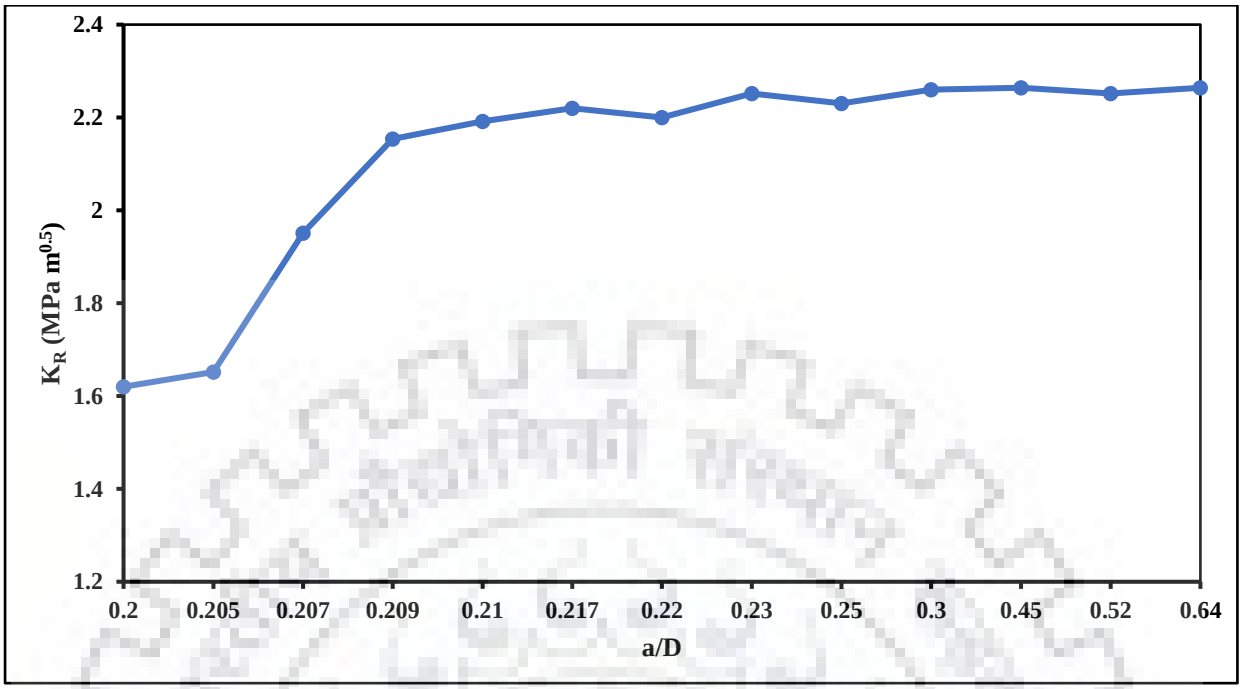

Figure 4.15: K_R curve for small beam

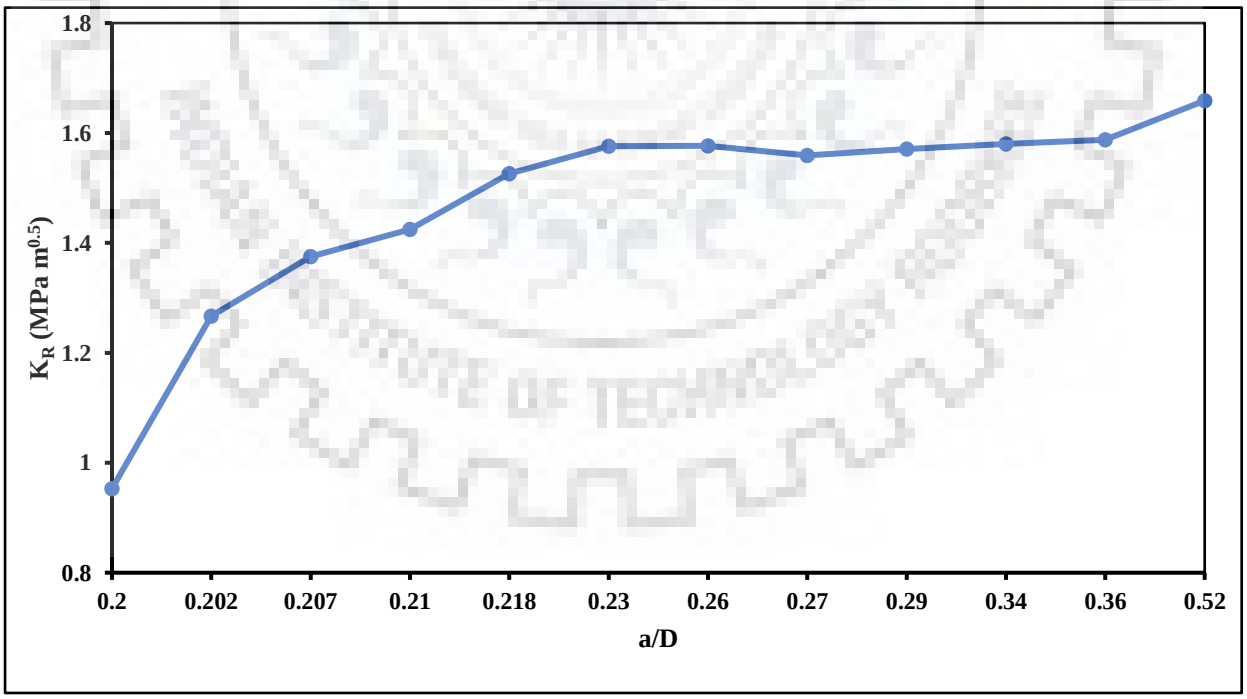

Figure 4.16: K_R curve for medium beam

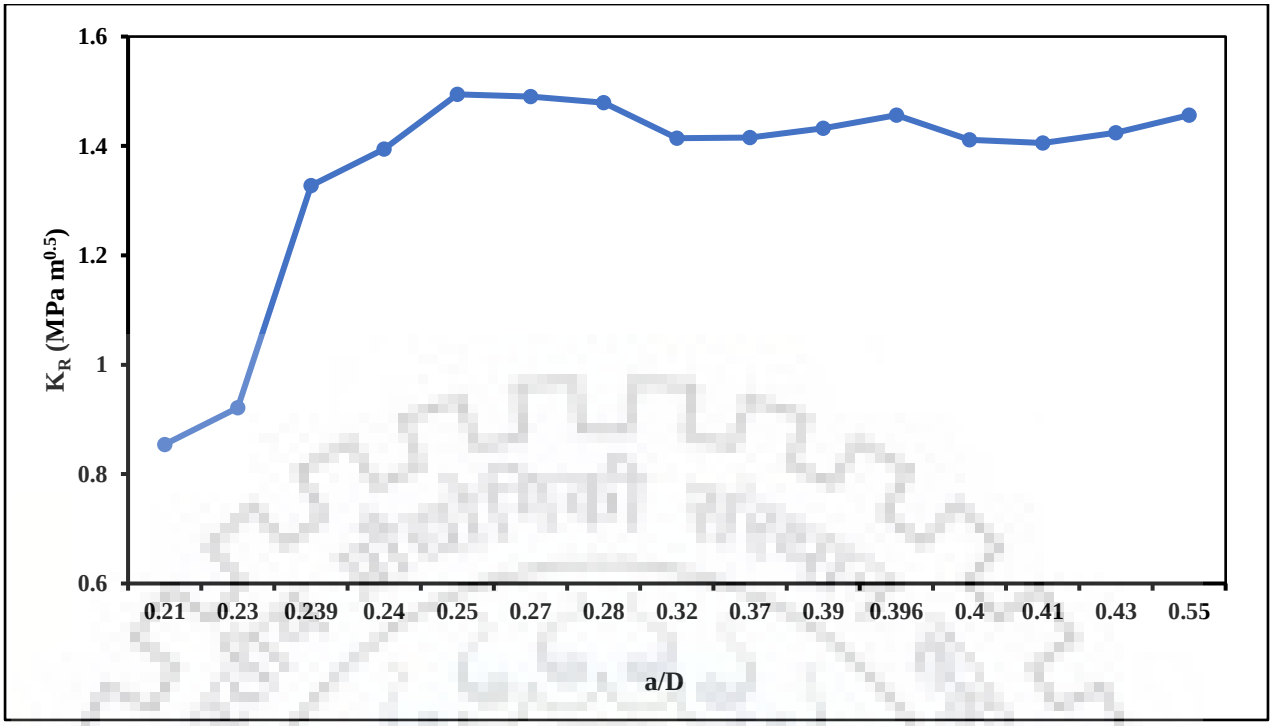

Figure 4.17: K_R curve for large beam

As we can clearly see from the above graphs of K_R curves that trend of all the curve is same. Crack extension resistance increases initially with the *a/D* ratio because of cohesive stress distribution within the crack. When cohesive stress reaches zero at crack tip, Stress free surface starts to propagate. The crack extension resistance tends to constant after the cohesive stress at crack tip becomes zero.

The shape of crack extension resistance in fatigue loading is same as that in static loading but its value is lower in fatigue loading as compared to static loading. The fracture resistance tends to become constant after cohesive stress reaches zero in both fatigue and static loading.

CHAPTER 5
CONCLUSION

In this report, the behavior and fracture process of concrete members under static and fatigue loading conditions have been investigated. Various numerical approaches have been used in this report for the calculation of fracture parameters by accounting all the change in fracture process zone throughout the fracture stage. Both linear asymptotic superposition assumption [6] and cohesive model [9] have been used for FPZ length calculation at various stages. For determination of K_R curve, initial and cohesive fracture toughness has been used. To understand the crack growth behavior under fatigue loading, Paris law has been adopted. In this report, a comparison has also been made between static and fatigue crack resistance and the various conclusions drawn from the results obtained are discussed below:

1. The fracture process zone first gradually increases and then decreases with the *a/D* ratio. When the fracture process zone is fully developed, it reaches to its maximum value.
2. The fully developed fracture process zone under monotonic loading has been determined as 30.71 mm, 59.85 mm and 120.47 mm for small, medium and large specimen.
3. The rate of crack growth initially has a deacceleration stage which is followed by an acceleration stage up to the failure. The rate of crack growth is independent of the specimen size.
4. The value of fracture toughness for small, medium and large beam has been determined as 1.54, 0.946 and 0.769 respectively.
5. The crack extension resistance initially increases with *a/D* ratio and then tends to keep constant after fracture process zone is fully developed, which shows that fracture process zone has a direct relationship with crack extension resistance.
6. The shape of the K_R curve is completely identical in both static and fatigue loading.
7. The value of crack extension resistance is lower under fatigue loading as compare to static loading.

REFERENCES

1. S. P. Shah, S. E. Swartz, and C. Ouyang, "*Fracture mechanics of concrete: Application of fracture mechanics to concrete, rock, and other quasi-brittle materials"*. John Wiley & Sons Inc., 1995.
2. S. P. Shah, S. V. Kolluru, E. F. O'Neil and J. S. Popovics: "Crack propagation in flexure fatigue of concrete" *Journal of engineering mechanics*, 126(9) (Sept 2000):891-898.
3. K. Otsuka, H. Date. "Fracture process zone in concrete tension specimen (2000)." *Engineering Fracture Mechanics*, 65 (2000) 111-131.
4. W. Yao, K. R. Wu, Z. J. Li. "Fracture Process Zone of Composite Materials as Concrete (1998)." *Fracture Mechanics of Concrete Structures, Proceedings of FRAMCOS-3*, 1998, p. 421-430
5. D. Wei, Z Xiangming, W. Zhimin, "on fracture process zone and crack extension resistance of concrete based on initial fracture toughness (2013)." *Construction and Building Materials*, 49:352-363.
6. F. Xu, Z. Wu, J. Zheng, Y. Zhao and K. Liu, "Crack Extension Resistance Curve of Concrete Considering Variation of FPZ Length" (2011). *Journal of Materials in Civil Engineering*, 23(5):703-710.
7. S. L. Xu, and H. W. Reinhardt, (1998). "Crack extension resistance and fracture properties of quasi-brittle softening materials like concrete based on the complete process of fracture." *Int. J. Fract.*, 92(1), 71–99.
8. N. Brake, and K. Chatti (2012). "Prediction of transient and steady-state flexural fatigue crack propagation in concrete using a cyclic R-Curve." *J. Eng. Mech.*, 10.1061/(ASCE)EM.1943-7889.0000338, 371–378.
9. L. Saucedo, C. Y. Rena, G. Ruiz. "Fully-developed FPZ length in quasi-brittle materials." *Int J Fract*, 2012; 178:97–112.
10. S. Bhowmik & S. Ray (2019). "An experimental Approach for Characterization of Fracture Process Zone in Concrete." *Engineering Fracture Mechanics*, 211. 10.1016/j.engfracmech.2019.02.026.
11. Y. S. Jenq, and S. P. Shah (1985b). "Two parameter fracture model for concrete." *J. Eng. Mech.*, 111(10), 1227–1241.

12. S. Shah, & J.M. Kishen. (2012). “Use of acoustic emissions in flexural fatigue crack growth studies on concrete.” *Engineering Fracture Mechanics*, 87. 36–47. 10.1016/j.engfracmech.2012.03.001.